



**HAL**  
open science

## Dissolved iodide in marine waters determined with Diffusive Gradients in Thin-films technique.

Josselin Gorny, Cyrielle Jardin, Olivier Diez, Josep Galceran, Alkiviadis Gourgiotis, Steffen Happel, Frederic Coppin, Laureline Fevrier, Caroline Simonucci, Charlotte Cazala

### ► To cite this version:

Josselin Gorny, Cyrielle Jardin, Olivier Diez, Josep Galceran, Alkiviadis Gourgiotis, et al.. Dissolved iodide in marine waters determined with Diffusive Gradients in Thin-films technique.. *Analytica Chimica Acta*, 2021, 1177, pp.338790. 10.1016/j.aca.2021.338790 . hal-03513525

**HAL Id: hal-03513525**

**<https://hal.science/hal-03513525>**

Submitted on 5 Jan 2022

**HAL** is a multi-disciplinary open access archive for the deposit and dissemination of scientific research documents, whether they are published or not. The documents may come from teaching and research institutions in France or abroad, or from public or private research centers.

L'archive ouverte pluridisciplinaire **HAL**, est destinée au dépôt et à la diffusion de documents scientifiques de niveau recherche, publiés ou non, émanant des établissements d'enseignement et de recherche français ou étrangers, des laboratoires publics ou privés.



Distributed under a Creative Commons Attribution - NonCommercial - NoDerivatives 4.0  
International License

# Journal Pre-proof

Dissolved iodide in marine waters determined with Diffusive Gradients in Thin-films technique

Josselin Gorny, Cyrielle Jardin, Olivier Diez, Josep Galceran, Alkiviadis Gourgiotis, Steffen Happel, Frédéric Coppin, Laureline Février, Caroline Simonucci, Charlotte Cazala

PII: S0003-2670(21)00616-4

DOI: <https://doi.org/10.1016/j.aca.2021.338790>

Reference: ACA 338790

To appear in: *Analytica Chimica Acta*

Received Date: 22 January 2021

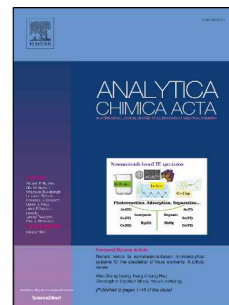
Revised Date: 15 June 2021

Accepted Date: 20 June 2021

Please cite this article as: J. Gorny, C. Jardin, O. Diez, J. Galceran, A. Gourgiotis, S. Happel, F. Coppin, L. Février, C. Simonucci, C. Cazala, Dissolved iodide in marine waters determined with Diffusive Gradients in Thin-films technique, *Analytica Chimica Acta*, <https://doi.org/10.1016/j.aca.2021.338790>.

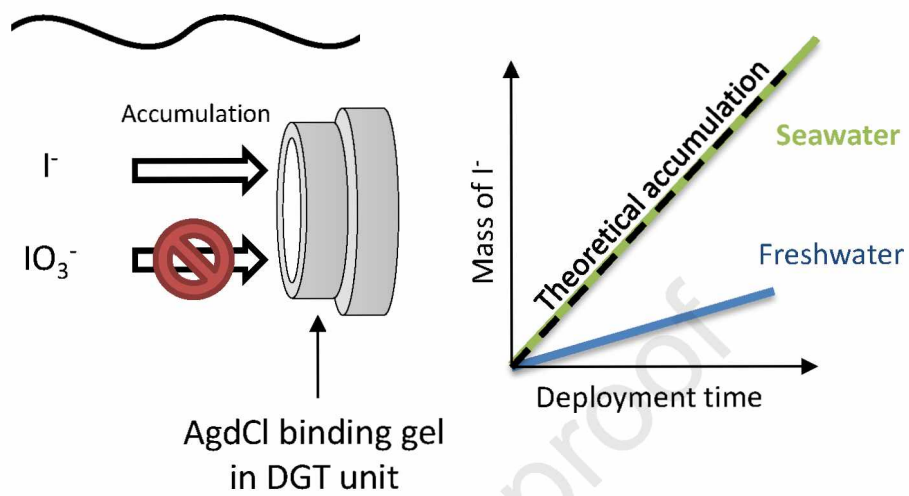
This is a PDF file of an article that has undergone enhancements after acceptance, such as the addition of a cover page and metadata, and formatting for readability, but it is not yet the definitive version of record. This version will undergo additional copyediting, typesetting and review before it is published in its final form, but we are providing this version to give early visibility of the article. Please note that, during the production process, errors may be discovered which could affect the content, and all legal disclaimers that apply to the journal pertain.

© 2021 Published by Elsevier B.V.



**Josselin Gorny:** Conceptualization, Methodology, Validation, Investigation, Resources, Writing - Original Draft, Review & Editing; **Cyrielle Jardin:** Methodology, Resources; **Olivier Diez:** Methodology, Resources; **Josep Galceran:** Conceptualization, Methodology, Validation, Formal analysis, Writing - Review & Editing; **Alkiviadis Gourgiotis:** Conceptualization, Methodology, Validation, Resources, Writing - Original Draft, Review & Editing; **Steffen Happel:** Conceptualization, Methodology, Resources; **Frédéric Coppin:** Conceptualization, Writing - Original Draft, Review & Editing; **Laureline Février:** Conceptualization, Writing - Original Draft, Review & Editing; **Caroline Simonucci:** Conceptualization, Funding acquisition, Writing - Original Draft, Review & Editing; **Charlotte Cazala:** Conceptualization, Project administration, Supervision, Writing - Original Draft, Review & Editing.

## Graphical abstract:



1 **Dissolved iodide in marine waters determined with Diffusive**  
2 **Gradients in Thin-films technique.**

3 Josselin Gorny<sup>a\*</sup>, Cyrielle Jardin<sup>a</sup>, Olivier Diez<sup>a</sup>, Josep Galceran<sup>b</sup>, Alkiviadis Gourgiotis<sup>a</sup>, Steffen  
4 Happel<sup>c</sup>, Frédéric Coppin<sup>d</sup>, Laureline Février<sup>d</sup>, Caroline Simonucci<sup>a,e</sup> and Charlotte Cazala<sup>a</sup>

5 <sup>a</sup> Institut de Radioprotection et de Sûreté Nucléaire (IRSN), PSE-ENV, SEDRE, LELI, Fontenay-aux-Roses, France

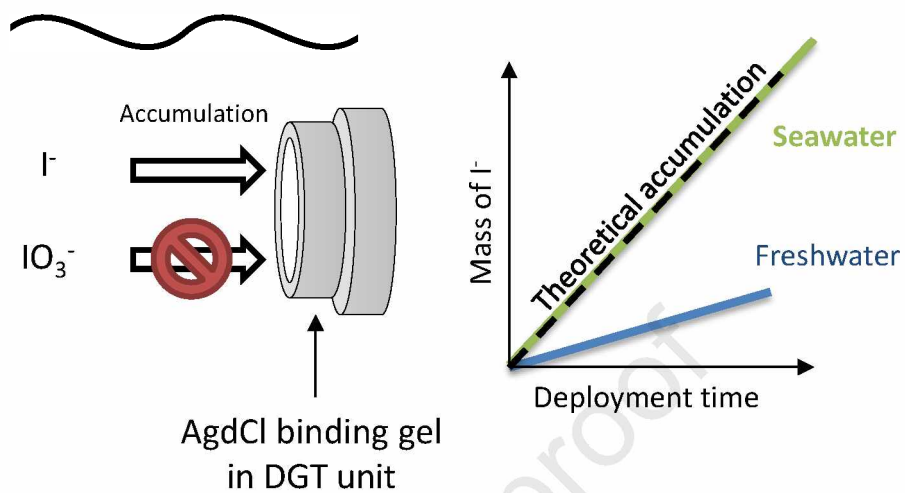
6 <sup>b</sup> Departament de Química, Universitat de Lleida and AGROTECNIO-CERCA, Rovira Roure 191, 25198, Lleida,  
7 Spain

8 <sup>c</sup> TrisKem International, Bruz, France

9 <sup>d</sup> Institut de Radioprotection et de Sûreté Nucléaire (IRSN), PSE-ENV, SRTE, LR2T, Cadarache, France

10 <sup>e</sup> present adress : Institut de Radioprotection et de Sûreté Nucléaire (IRSN), PSE-ENV, SIRSE, LER-NORD

11 \* Corresponding author: [josselin.gorny@irsn.fr](mailto:josselin.gorny@irsn.fr);

12 **Graphical abstract:**

13

14

**15 Keywords:**

16 Iodine; Redox speciation; Diffusive Gradients in Thin-films; Time-series experiment; Laboratory  
17 validation; Iodide; Marine waters.

**18 Highlights:**

- 19 - A new DGT binding gel is proposed for selective iodide sampling.
- 20 - The diffusion coefficient of I species through agarose diffusive gel is reported.
- 21 - A DGT equation is developed to simultaneously consider DBL and kinetic effects.
- 22 - The method was successfully applied to measure iodide concentrations in seawater.

**23 Abstract**

24 For the first time, Diffusive Gradient in Thin-films (DGT) focuses on the inorganic iodine species  
25 iodate ( $\text{IO}_3^-$ ) and iodide ( $\text{I}^-$ ). A silver-doped Cl resin ( $\text{AgdCl}$ ), which is known to selectively  
26 accumulate  $\text{I}^-$ , was used to make a binding gel. Laboratory investigations were designed to verify  
27 the suitability of the  $\text{AgdCl}$ -DGT method to measure the total  $\text{I}^-$  concentration in environmental  
28 waters. Total recovery of  $\text{I}^-$  was obtained using an elution solution containing  $100 \text{ mmol L}^{-1}$   
29 KCN. DGT validation experiments in  $10 \text{ mmol L}^{-1}$  NaCl showed linear accumulation of  $\text{I}^-$  over  
30 time, contrary to  $\text{IO}_3^-$ , thus confirming the selectivity of  $\text{AgdCl}$ -binding gel. The  $\text{AgdCl}$ -DGT  
31 measurement of total  $\text{I}^-$  concentration was independent of pH (4.5 – 8.8) and was not impacted by  
32 the presence of bicarbonate ( $1\text{-}5 \text{ mmol L}^{-1}$ ). Finally, the performance of  $\text{AgdCl}$ -DGT samplers  
33 were tested in two continental waters and a synthetic seawater. The  $\text{AgdCl}$ -DGT samplers  
34 measured 27-33 % of the total  $\text{I}^-$  concentration in the two continental waters up to 24 h of  
35 deployment time, whereas the  $\text{AgdCl}$ -DGT response retrieved the total  $\text{I}^-$  concentration in  
36 seawater up to 72 h ( $106 \pm 7 \%$ ). The difference in DGT response was attributed to the low ionic  
37 strength of the two continental waters, limiting the application of  $\text{AgdCl}$ -DGT method to media  
38 with higher ionic strength.

## 39 1. Introduction

40 Natural iodine (I) is composed of the stable isotope  $^{127}\text{I}$  and the long-lived beta-emitting  
41 radioisotope  $^{129}\text{I}$  ( $t_{1/2} = 15.7 \times 10^6$  years), which is mainly produced by nuclear activities (uranium  
42 and released plutonium fission in the environment especially by fuel reprocessing plants) [1].  
43 Indeed, the  $^{129}\text{I}/^{127}\text{I}$  ratio can reach  $10^{-8}$ - $10^{-6}$  in marine waters at the vicinity (<50 km) of  
44 European fuel reprocessing plants, values significantly higher in comparison of the representative  
45 ratio commonly considered in the hydrosphere ( $1.5 \times 10^{-12}$ ) [2]. The behaviour and the transfer  
46 between compartments of  $^{129}\text{I}$  highly depends on its speciation, which thus must be taken into  
47 account to assess short- and long-term consequences of  $^{129}\text{I}$  releases.

48 Iodine is occurring as a redox sensitive trace element in environment with concentration  
49 generally lower than  $100 \mu\text{g L}^{-1}$  (for the stable isotope) [3-8]. Data on its speciation are generally  
50 restricted to surface seawater environment, in which the most common I species found are iodide  
51 ( $\text{I}^-$ ), iodate ( $\text{IO}_3^-$ ) and dissolved organic iodine [9-12]. In contrast, few data are available on the  
52 behavior of I species at the water-sediment interface. These ones are mainly documented in  
53 marine environment, where total I concentrations are the most elevated [13-15], reflecting the  
54 high level of difficulty to analyze its speciation at very low concentration in continental  
55 environment. One solution to overcome these difficulties in aquatic environment is to use passive  
56 samplers, which concentrate the analyte of interest. Here, we propose to use the Diffusive  
57 Gradient in Thin film (DGT) technique, which is a passive sampling technique [16, 17]. The  
58 DGT sampling allows the preconcentration of the target species, leading to the improvement of  
59 their determination by chemical analysis. Nowadays, the development of DGT method permits to  
60 partially or totally access the redox speciation of the following elements: As [18-20], Br [21], Cr



61 [22-24], Hg [25, 26], N [27-29], P [30], S [31, 32], Sb [33, 34], Se [35] and V [36]. But, to best of  
62 our knowledge there is no DGT method for I species.

63 In this study, we have investigated the possibility to develop a binding gel able to accumulate  
64 specifically I. The silver-doped Cl resin, developed by Triskem international  
65 (<https://www.triskem-international.com/>) has been tested as an adsorbent phase. It was already  
66 used to preconcentrate I in extraction chromatography, due to its strong interaction with silver  
67 [37, 38]. Laboratory validation experiments were designed: (i) to find an inert filter membrane  
68 and diffusive gel to make DGT samplers; (ii) to define the selectivity of the new binding gel for  
69 inorganic I species in the presence of potential competing ions ( $\text{Cl}^-$  and  $\text{SO}_4^{2-}$ ) from batch  
70 experiments; and (iii) to evaluate its performance in DGT in synthetic and natural matrices  
71 (selectivity, effect of pH, intrinsic capacity, carbonate interferences, continental and marine  
72 waters).

## 73 2. Experimental section

### 74 2.1. Reagents, materials and solutions

75 All the solutions were prepared with deionized water (18.2 M $\Omega$  cm resistivity, Milli-Q water,  
76 Millipore). The polypropylene plastic containers were acid-cleaned in 1.5 mol L<sup>-1</sup> HNO<sub>3</sub> solution  
77 over 24 h, then rinsed several times with deionized water prior to DGT sampler deployment. The  
78 following chemicals were used: agarose (Bio-rad), AgNO<sub>3</sub> (VWR), KCN (VWR, normapur), HCl  
79 (Merck, Emsure 37 %), HNO<sub>3</sub> (VWR Chemicals, Normapur 68 %), KI (VWR, normapur), NaCl  
80 (Merck, suprapur), Na<sub>2</sub>SO<sub>4</sub> (Merck, suprapur), NaOH (Merck, normapur), NH<sub>3</sub> (Merck, utrapur  
81 20 %), cellulose acetate (CA; Sartorius, 0.45  $\mu\text{m}$  pore size), polycarbonate (PC; Pall, 0.45  $\mu\text{m}$   
82 pore size), polyester sulfone (PES; Pall, 0.45  $\mu\text{m}$  pore size) and polyvinylidene fluoride filter  
83 discs (PVDF; Merck Durapore, 0.45  $\mu\text{m}$  pore size). Concerning standard solutions we used IO<sub>3</sub><sup>-</sup>

84 solution ( $1 \text{ g L}^{-1}$ ; conditioned in deionized water; VWR), anions chromatography solution  
85 including  $\text{Cl}^-$ ,  $\text{Br}^-$ ,  $\text{NO}_3^-$ ,  $\text{NO}_2^-$ ,  $\text{I}^-$ ,  $\text{SO}_4^{2-}$  and  $\text{PO}_4^{3-}$  ( $100 \text{ mg L}^{-1}$ ; conditioned in deionized water;  
86 VWR), acidified Te and Pt solution ( $1 \text{ g L}^{-1}$ ; VWR).

## 87 **2.2. Gel preparation and DGT assembly**

88 Agarose (AGE) and agarose-polyacrylamide (APA) diffusive gel were made as in [39] and [40],  
89 respectively. The diffusive gel was stored in  $10^{-2} \text{ mol L}^{-1}$  ultrapure NaCl solution. The thickness  
90 of diffusive gel was  $800 \mu\text{m}$ , value controlled with an optical microscope as in [39]. The binding  
91 layer was constituted by an  $\text{Ag}^+$  loaded Cl resin (AgdCl) embedded in agarose gel. The Cl resin  
92 ( $50 - 100 \mu\text{m}$ ) was provided by Triskem international. The AgdCl resin was prepared by  
93 contacting  $1 \text{ g}$  of the Cl resin with  $10 \text{ mL}$  of  $10 \text{ mg mL}^{-1}$   $\text{AgNO}_3$  solution in an orbital shaker  
94 over a period of 2 hours. During this step, the color of the Cl resin changed from white to beige.  
95 Then, the AgdCl resin was rinsed with  $80 - 100 \text{ mL}$  of ultrapure water in a polypropylene  
96 column connected to a vacuum box (Triskem international). The interstitial water was eliminated  
97 by increasing pressure to the maximum in the vacuum box. Finally, the AgdCl resin was mixed  
98 with  $10 \text{ mL}$  of  $1.5\%$  (w/v) hot agarose solution. This mixture was, then, poured between two hot  
99 glass plates ( $50 \text{ }^\circ\text{C}$ ) separated by a  $0.8 \text{ mm}$  Teflon plastic spacer at room temperature for at least  
100 30 minutes. Once binding gel was completely polymerized, it was removed from the glass plates,  
101 rinsed three times to remove unreacted reagents (during 24 hours), and placed into ultrapure  
102 water bath (2 weeks maximum). The AgdCl binding gel, the diffusive gel and the filter were then  
103 assembled in a piston-type ABS DGT sampler with a sampling area of  $3.14 \text{ cm}^2$  (DGT Research  
104 Ltd).

### 105 **2.3. Analytical procedures**

106 Total iodine concentration was measured by Inductively Coupled Plasma –Mass Spectrometry  
107 (ICP-MS; Agilent 8800). The ICP-MS was equipped with a PFA concentric nebulizer (ESI), a  
108 double-pass PFA spray chamber cooled at 2°C, a PFA T-piece with an internal solution, a  
109 demountable torch with a sapphire injector, and Ni cones. ICP-MS spectrometer was calibrated  
110 using freshly standard solutions following a matrix-matching procedure between samples and  
111 standard solutions (*i.e.*, 150 mmol L<sup>-1</sup> NH<sub>3</sub> for basified water samples and 10 mmol L<sup>-1</sup> KCN for  
112 eluent solution). Internal standard (<sup>125</sup>Te in 150 mmol L<sup>-1</sup> NH<sub>3</sub> for basified water samples [4] or  
113 <sup>195</sup>Pt (element selected due to its stability in cyanide media [41]) in 10 mmol L<sup>-1</sup> KCN for eluent  
114 solution) was used to correct for instrumental signal drift of ICP-MS over time; the concentration  
115 of the internal standard concentrations was adjusted to obtain 50000 – 70000 cps at m/z 125 or  
116 195.

117 Speciation measurement was carried out on filtered water samples by chromatographic separation  
118 using a Metrohm 940 Professional IC Vario Ion Chromatography (IC) system. The  
119 chromatographic system was equipped with Metrosep A Supp 10 guard column (4.6 µm particle  
120 diameter, 2 mm i.d. × 5 mm) coupled with a Metrosep A Supp 10 analytical column (4.6 µm  
121 particle diameter, 2 mm i.d. × 250 mm), a 20 µL PEEK injection loop, a thermostatic column  
122 oven set at 35 ± 0.1°C, a mobile phase containing 50 mmol L<sup>-1</sup> NH<sub>4</sub>NO<sub>3</sub> (pH 5.5 ± 0.1), a PEEK  
123 capillary (15 cm) connecting the column outlet to the nebulizer of ICP-MS. The flow rate of  
124 mobile phase was fixed at 250 µL min<sup>-1</sup>. Standard solutions were freshly prepared in deionized  
125 water. The chromatographic conditions were developed in partnership with Metrohm France (see  
126 section S1-S5, Figure S1-S4, Table S1 and S2 in supplementary information).

127 Inductively Coupled Plasma – Optical Emission Spectrometry (ICP-OES; Thermo iCAP<sup>TM</sup> 7400,  
128 axial view) was used to evaluate the uptake capacity of AgdCl-DGT sampler for inorganic I  
129 species (section 2.5.5). Standard solutions were prepared as for ICP-MS calibration.

## 130 **2.4. Experiments with DGT components**

### 131 **2.4.1. Reactivity of filter, diffusive gel and DGT plastic holder**

132 Before performing DGT experiments, the reactivity of common diffusive gel (AGE and APA),  
133 filter membrane (CA, PC, PES and PVDF) and ABS-DGT plastic holder was tested regarding  
134 inorganic I species. Batch experiments were performed with each component immersed in 20 ml  
135 of solution containing 25  $\mu\text{g L}^{-1}$  of  $\text{IO}_3^-$  or  $\text{I}^-$ . Experimental solution was vigorously shaken for 24  
136 h using an orbital shaker. Filtered batch solutions were, then, basified with ultrapure  $\text{NH}_3$  at 150  
137  $\text{mmol L}^{-1}$  before elemental analysis. The recovery of inorganic I species ( $R$ , %) in immersion  
138 solution was calculated using the following equation (Eq. 1).

$$R = \frac{M_f}{M_i} \times 100 \quad \text{Eq. 1}$$

139 where  $M_i$  and  $M_f$  are respectively the initial and final mass ( $\mu\text{g}$ ) of inorganic I species in  
140 deployment solution.

### 141 **2.4.2. Reactivity of binding gel**

142 The first step was devoted to define the uptake capacities of inorganic I species by the AgdCl-  
143 binding gel to confirm the possibility of using it as a new DGT binding gel. The affinity of  
144 inorganic I species with AgdCl binding gels were examined by batch experiments with 20 mL of  
145 solution containing 100  $\mu\text{g L}^{-1}$  of  $\text{IO}_3^-$  or  $\text{I}^-$  where one binding gel was immersed to float freely.  
146 The experiments were performed at various ionic strength ( $[\text{NaCl}]$  or  $[\text{Na}_2\text{SO}_4] = 1 - 500 \text{ mmol}$   
147  $\text{L}^{-1}$ ;  $\text{pH } 5.5 \pm 0.1$ ). The solution was vigorously shaken for 24 h with an orbital shaker. Filtered

148 batch solutions were, then, basified with ultrapure  $\text{NH}_3$  at  $150 \text{ mmol L}^{-1}$  before elemental  
149 analysis. The uptake factor ( $f_u$ , %, Eq. 2) was calculated from the initial mass of inorganic I  
150 species in the deployment solution ( $M_i$ ,  $\mu\text{g}$ ), and the remaining mass of iodine species ( $M_f$ ,  $\mu\text{g}$ ):

$$f_u = \frac{M_i - M_f}{M_i} \times 100 \quad \text{Eq. 2}$$

151 The second step was to find a suitable eluent solution that could quantitatively recover the  
152 inorganic I species from AgdCl-binding gel. As cyanides are known to form strong complexes  
153 with  $\text{Ag}^+$  [41], the AgdCl-binding gel was immersed for 24 h in 3 mL of KCN solution ( $0.1 - 100$   
154  $\text{mmol L}^{-1}$ ) containing  $100 \mu\text{g L}^{-1}$  of inorganic I species. The recovery of inorganic I species in  
155 KCN solution was calculated using Eq. 1.

## 156 **2.5. Laboratory evaluation of DGT performances**

157 This section focuses on the laboratory evaluation of AgdCl-DGT method in deployment  
158 solutions. The general experimental setup and calculations are firstly described, followed-up by a  
159 description of classical tests to specify the performances of the new DGT binding gel in terms of  
160 selectivity, pH influence, uptake capacity and deployment in natural matrices.

### 161 **2.5.1. Experimental setup and calculations**

162 All DGT experiments were performed in polypropylene containers (30 L). After equilibration of  
163 the deployment solution with the atmosphere during at least 24 hours, AgdCl-DGT samplers  
164 were deployed at specific time interval. The temperature and pH were monitored. Prior to the  
165 retrieval of the AgdCl-DGT, aliquots of the deployment solution were taken, filtered through  
166 acetate cellulose filter ( $0.45 \mu\text{m}$ ), then basified with ultrapur  $\text{NH}_3$  at  $150 \text{ mmol L}^{-1}$  before  
167 elemental analysis. Mean values of temperature, pH, concentration of inorganic I species are

168 included in the figures and uncertainties are expressed as the standard deviation of the variation  
 169 of these parameters during the experiments.

170 The accumulated mass of inorganic I species by AgdCl-binding gel ( $M_{DGT}$ , ng) was calculated  
 171 using Eq. 3.

$$M_{DGT} = \frac{C_e \times (V_{KCN} + V_{gel})}{f_e/100} \quad \text{Eq. 3}$$

172 where  $C_e$  is the eluted concentration of I in the selected elution solution ( $\text{ng mL}^{-1}$ ),  $V_{KCN}$  the  
 173 eluent solution volume (mL),  $V_{gel}$  the volume of the AgdCl-binding gel (mL) and  $f_e$  the eluent  
 174 factor (%).

175 To determine the experimental DGT performances, the theoretical mass of inorganic I species  
 176 ( $M_{th1}$ , ng) accumulated in the AgdCl-binding gel was calculated using Eq. 4, which is based on  
 177 the well-established DGT equation [17].

$$M_{th1} = \frac{C_I \times A_P \times t}{\left(\frac{\delta^{mdl}}{D^{mdl}}\right)} \quad \text{Eq. 4}$$

178 where  $C_I$  is the concentration of  $\text{IO}_3^-$  or  $\text{I}^-$  in the deployment solution ( $\text{ng cm}^{-3}$ ),  $D^{mdl}$  the diffusion  
 179 coefficient of each inorganic I species (in the material diffusion layer) obtained by the diffusion  
 180 cell method ( $\text{cm}^2 \text{s}^{-1}$ ),  $A_P$  the geometric area of the DGT device window ( $3.14 \text{ cm}^2$ ),  $t$  the  
 181 deployment time (s) and  $\delta^{mdl}$  the thickness of the diffusive gel plus the filter membrane ( $0.093$   
 182 cm).

### 183 **2.5.2. Selectivity and determination of the effective diffusion coefficient**

184 The accumulation of inorganic I species was investigated by deploying five sets of triplicate  
 185 AgdCl-DGT samplers in 8 L of  $30 \mu\text{g L}^{-1}$   $\text{IO}_3^-$  or  $\text{I}^-$  (prepared in  $10^{-2} \text{ mol L}^{-1}$  NaCl at  $\text{pH } 5.5 \pm$

186 0.1). Triplicate AgdCl-DGT samplers were removed at around 2, 4, 6, 8 and 10 h. In condition  
 187 where all inorganic I species are labile, if a linear accumulation is observed over time with  $R^2 >$   
 188 0.95, the effective diffusion coefficient ( $D^{\text{eff}}$ ,  $\text{cm}^2 \text{s}^{-1}$ ) of considered inorganic I species value can  
 189 be calculated using Eq.5.

$$D^{\text{eff}} = \frac{\alpha \times \delta^{\text{mdl}}}{C_1 \times A_p} \quad \text{Eq. 5}$$

190 where  $\alpha$  is the slope of linear regression of the mass accumulated of considered inorganic I  
 191 species over time ( $\text{ng s}^{-1}$ ).

192 To check the selectivity of AgdCl-DGT samplers for both inorganic I species, complementary  
 193 experiments were carried out in 8 L of  $10^{-2} \text{ mol L}^{-1}$  NaCl at  $\text{pH } 5.5 \pm 0.1$  containing inorganic I  
 194 species with different weight ratio  $[\text{I}^-] / [\text{IO}_3^-]$  (0, 0.4, 0.9, 1.7, 2.4 and 4.6; values obtained after  
 195 speciation control by IC-ICP-MS). The concentration of  $\text{IO}_3^-$  was fixed at a value close to  $20 \mu\text{g}$   
 196  $\text{L}^{-1}$ , whereas  $\text{I}^-$  concentrations varied. Triplicate AgdCl-DGT samplers were deployed for 10 h.

### 197 **2.5.3. Effect of pH**

198 The effect of pH on  $\text{I}^-$  accumulation was evaluated by deploying four AgdCl-DGT samplers in  
 199 8 L of  $20 \mu\text{g L}^{-1}$   $\text{I}^-$  (prepared in  $10^{-2} \text{ mol L}^{-1}$  NaCl at  $\text{pH } 5.5 \pm 0.1$ ) for 10 h. The pH selected for  
 200 these experiments were the following: 4.5, 5.5, 6.6, 7.6 and 8.8. Acidification at pH 4.5 was  
 201 performed using  $6 \text{ mol L}^{-1}$  HCl solution. A pH titrator (Metler Toledo), equipped with a DGi115  
 202 glass electrode (Metler Toledo) and dilute NaOH solution were used to control and adjust the pH  
 203 of the deployment solutions for  $\text{pH} > 6$ .

#### 204 **2.5.4. Effect of bicarbonate**

205 The effect of bicarbonate was tested by deploying five sets of triplicate AgdCl-DGT samplers in  
206 8 L of 10 mmol L<sup>-1</sup> NaCl solution containing either 1 or 5 mmol L<sup>-1</sup> of NaHCO<sub>3</sub>. The  
207 concentration of I<sup>-</sup> was close to 30 µg L<sup>-1</sup> in the two deployment solutions. Triplicate DGT  
208 samplers were removed after 4, 6, 8, 10 and 24 h.

#### 209 **2.5.5. Binding capacity of AgdCl-DGT samplers**

210 The intrinsic binding capacity of AgdCl-binding gel was investigated by deploying six sets of  
211 triplicate AgdCl-DGT samplers in 8 L of around 20 mg L<sup>-1</sup> I<sup>-</sup> (prepared in 10<sup>-2</sup> mol L<sup>-1</sup> NaCl at  
212 pH 5.5 ± 0.1). Triplicate DGT samplers were removed after 2, 4, 6, 8, 24 and 28 h.

#### 213 **2.5.6. Time-series experiment in natural and synthetic matrix**

214 To determine the performances of AgdCl-DGT in environmentally relevant matrices, AgdCl-  
215 DGT samplers were deployed in 8 L of Vittel®, Volvic® or synthetic seawater. The Vittel® and  
216 Volvic® continental waters were spiked with I<sup>-</sup> at around 25 µg L<sup>-1</sup>, and the synthetic seawater at  
217 100 µg L<sup>-1</sup> (a higher level, due to important dilution before elemental and speciation  
218 measurements). Physico-chemical characteristics of drinking waters are reported in Table 1.  
219 Triplicate AgdCl-DGT samplers were removed after a defined deployment time (2 – 72 h). For  
220 samplers deployed in seawater, each AgdCl-binding gel was rinsed in 5 mL of ultrapure water for  
221 2 h to remove unbound salts.



## 222 **3. Results and discussion**

### 223 **3.1. Experiments with DGT components**

#### 224 **3.1.1. Reactivity of filter, diffusive gel and DGT plastic holder**

225 The ABS DGT holder did not react with  $\text{IO}_3^-$  or  $\text{I}^-$  ( $R = 101-102\%$ ). All filter membranes (CA,  
226 PC, PES or PVDF) and diffusive gels (AGE or APA) tested did not accumulate inorganic I  
227 species ( $R = 98-102\%$ ). For more details, data are available in Figure S5 in the supplementary  
228 information. To make DGT samplers for inorganic I species, there is consequently no limitation  
229 using a specific combination of filter membrane and diffusive gel rather than another. This is not  
230 the case when working, for example, with mercury (which adsorbs on APA diffusive gel) [42-  
231 44]. For the next experiments, the CA filter membrane and AGE diffusive gel were used as  
232 standard DGT components.

#### 233 **3.1.2. Reactivity of binding gel**

234 The uptake efficiency of the AgdCl-binding gel disc is shown as a function of NaCl or  $\text{Na}_2\text{SO}_4$   
235 concentration in Figure 1 (A) and (B), respectively. Immersion time was 24 h.  $\text{I}^-$  was totally  
236 accumulated by the AgdCl-binding gel without being impacted by the NaCl and  $\text{Na}_2\text{SO}_4$   
237 concentrations in the immersion solution ( $f_u > 98\%$ ). Consequently, chloride ( $\text{Cl}^-$ ) and sulfate  
238 ( $\text{SO}_4^{2-}$ ) ions are not a competing ion for the uptake of  $\text{I}^-$  by the AgdCl-binding gel for  
239 concentration up to  $500\text{ mmol L}^{-1}$ . The uptake factor by AgdCl-binding gel is very limited for  
240  $\text{IO}_3^-$  ( $f_u < 15\%$ ). For these batch experiments, no speciation controls were done. The aim was  
241 only to roughly determine the selectivity of AgdCl-binding gel. It might be that some redox  
242 interconversion of  $\text{IO}_3^-$  to  $\text{I}^-$  could explain the low  $\text{IO}_3^-$  uptake in NaCl media. In any case, these  
243 results open up the possibility to develop a DGT method selective to  $\text{I}^-$ . This hypothesis will be

244 tested through DGT experiments in the section 3.2, in which the speciation of I was checked in  
245 each deployment solution.

246 Then, the binding dynamics of I by AgdCl-binding gel disc was studied in 10 mmol L<sup>-1</sup> NaCl  
247 and Na<sub>2</sub>SO<sub>4</sub> immersion solution as shown Figure 1 (C). The mass of I bound to AgdCl-binding  
248 gel disc increased steeply at the first 10-20 min, followed by a slow increase later on. The binding  
249 rates at 5 min are 0.68 and 1.08 ng s<sup>-1</sup> cm<sup>-2</sup> for NaCl and Na<sub>2</sub>SO<sub>4</sub> immersion solution,  
250 respectively. These values are much greater than DGT fluxes (0.022 ng s<sup>-1</sup> cm<sup>-2</sup>) calculated  
251 through a 0.093 cm a diffusive layer (typically used in DGT assemblies), the diffusion coefficient  
252 of I in free water (Table 2), and a deployment solution containing the same concentration of I at  
253 25°C. It shows that I binding to AgdCl-binding gel can be high enough to satisfy DGT uptake.  
254 Furthermore, Figure 1 (C) indicates a lower uptake for the lower ionic strength (10 mmol L<sup>-1</sup> for  
255 NaCl solution vs 30 mmol L<sup>-1</sup> for Na<sub>2</sub>SO<sub>4</sub> solution), which was not observable in previous  
256 experiments due to long immersion time (24 h). This is probably linked to the nature of AgdCl-  
257 resin. One possible mechanism is hypothesized next. Once I, Cl<sup>-</sup> and SO<sub>4</sub><sup>2-</sup> enter into the AgdCl-  
258 resin bead, these anions react with Ag<sup>+</sup> to form precipitates. The precipitation of Ag<sub>2</sub>SO<sub>4</sub> and  
259 AgCl does not hinder the formation of AgI because of its lower solubility product constant value  
260 (pK<sub>sp</sub> = 4.8, 9.75 and 16.1 for Ag<sub>2</sub>SO<sub>4</sub>, AgCl and AgI precipitates [41], respectively). This was  
261 also confirmed by our previous batch experiments showing total uptake of I by AgdCl-binding  
262 gel disc whatever the concentration of NaCl and Na<sub>2</sub>SO<sub>4</sub> in immersion solution. Nevertheless, the  
263 penetration of the negatively charged I inside the AgdCl-resin bead could be restricted due to  
264 residual negatively charged sites on the AgdCl-resin. The electrostatic potential difference  
265 (between the resin and the solution) increases with decreasing of ionic strength [45-48], and I  
266 tends to be excluded from the AgdCl-resin. So, less accumulation will follow in low ionic

267 strength. This hypothetical mechanism would explain why a faster uptake was observed in  
268  $\text{Na}_2\text{SO}_4$  immersion solution than in the NaCl (Figure 1(C)) one with the same analyte  
269 concentration, but different ionic strength. These results point out to a potential limitation of the  
270 use the AgdCl-DGT method. In section 3.2, experiments will be designed to better understand how  
271 to use the AgdCl-DGT method, but also to check whether this decreased accumulation at lower  
272 ionic strength is negligible or not.

273 To define the eluent solution, the recovery of  $\Gamma$  from AgdCl-binding gel was tested using 3 mL of  
274 KCN solution at different concentrations (0.1 – 100  $\text{mmol L}^{-1}$ ), as shown in Figure 2. Total  
275 recovery of  $\Gamma$  was obtained for KCN concentration higher than 10  $\text{mmol L}^{-1}$  ( $R = 101 - 103 \%$ ).  
276 The AgdCl-binding gel disc became white (initial color of Cl resin) when using 100  $\text{mmol L}^{-1}$   
277 KCN, suggesting that Ag is totally removed in the eluent solution and there is no  $\Gamma$  left in the  
278 AgdCl binding gel. Hence, this concentration was used to totally elute  $\Gamma$  from AgdCl binding gel.  
279 To prevent signal suppression of ICP-MS linked to high potassium concentration, the eluent  
280 solutions were diluted at least 10 fold with deionized water. Finally, no elution factor is needed to  
281 calculate the mass of  $\Gamma$  accumulated by the AgdCl-binding gel ( $f_e = 100 \%$  in Eq. 3).  
282 Furthermore, the AgdCl-DGT blank values for  $\Gamma$  species were 5 ng ( $n = 10$ ) following this  
283 elution procedure. This blank value of AgdCl-DGT method is low enough to measure the low  
284 concentration of  $\Gamma$  in environmental waters.

## 285 **3.2. DGT experiments**

### 286 **3.2.1. Speciation and lability**

287 To be sure of the stability of inorganic I species in deployment solution, speciation was checked  
288 with IC-ICP-MS measurements during DGT experiment. The concentration of inorganic I species

289 was relatively stable over time in each deployment solution with RSD < 5 %, confirming that  
290 there is no redox interconversion in these DGT experiments. Concerning the lability of inorganic  
291 I species, speciation calculations were performed with PHREEQC version 3  
292 (<https://www.usgs.gov/software/phreeqc>) with the thermodynamic database ThermoChimie  
293 version 9b0 developed by Andra (<http://www.thermochimie-tdb.com/>) [49, 50]. Input data were  
294 the concentrations of each component in deployment solution. Atmosphere-water equilibrium  
295 with CO<sub>2</sub> was also assumed. pH and temperature was also introduced. Whatever the simulated  
296 deployment solution, IO<sub>3</sub><sup>-</sup> and I<sup>-</sup> were mainly present as free ions (> 95 %). Hence, it was  
297 considered that inorganic I species were totally available for the AgdCl-DGT samplers.

### 298 3.2.2. Selectivity of AgdCl-DGT method

299 Time-series experiments were used to characterize the selectivity of AgdCl-DGT samplers for  
300 inorganic I species (Figure 3). AgdCl-DGT samplers were deployed up to 10 h in the presence of  
301 either IO<sub>3</sub><sup>-</sup> or I<sup>-</sup> (~ 30 µg L<sup>-1</sup>). The mass of IO<sub>3</sub><sup>-</sup> stabilized at 14 ± 2 ng after 2 h of deployment  
302 time, which coincides with the amount for equilibrium ( $[\text{IO}_3^-]_{\text{solution}} \times V_{\text{gel}} \sim 12 \text{ ng}$  with  $V_{\text{gel}} = 0.42$   
303 ± 0.03 mL), assuming no electrostatic effect. This indicated that IO<sub>3</sub><sup>-</sup> was not trapped over time in  
304 the AgdCl binding gel. Consequently, this DGT method should not suffer from any IO<sub>3</sub><sup>-</sup>  
305 interference. Selectivity control was performed using a deployment solution containing the two  
306 inorganic I species, and results are discussed later on. A good linear regression was obtained  
307 between the accumulated mass of I<sup>-</sup> and the deployment time of DGT samplers ( $R^2 = 0.994$ ),  
308 confirming previous results on the selectivity of AgdCl-binding gel (section 3.1.2). The slope of  
309 linear fitting was used to calculate  $D^{\text{eff}}$  according to Eq. 5. The  $D^{\text{eff}}$  value for I<sup>-</sup> was 1.20 10<sup>-5</sup> cm<sup>2</sup>  
310 s<sup>-1</sup> (RSD = 6 %) at 25°C value. Complementarily, the diffusion cell method was used to measure  
311 the diffusion coefficient of each inorganic I species in hydrogel alone ( $D^{\text{gel}}$ ) and with the addition

312 of a filter ( $D^{\text{mdl}}$ ). Experimental details are presented in section S6, and the diffusion cell is shown  
 313 in Figure S6. The concentration of  $\text{IO}_3^-$  or  $\Gamma$  were both constant in the source solution during each  
 314 diffusion cell experiments with a RSD  $< 4\%$ , confirming the non-adsorption of inorganic I  
 315 species by the components and the walls of diffusive cell. Linear accumulation of  $\text{IO}_3^-$  or  $\Gamma$  in the  
 316 acceptor compartment was observed over time ( $R^2 = 0.997-0.999$ ; Figure S7), and each slope was  
 317 used to calculate the diffusion coefficient of inorganic I species according to Eq. S1. Results are  
 318 displayed in Table 2. The diffusion of inorganic I species is slightly higher in hydrogel than in  
 319 pure water ( $D^{\text{gel}} / D^{\text{w}} \sim 110\%$ ). Slower diffusion of  $\text{IO}_3^-$  and  $\Gamma$  was observed with the addition of  
 320 filter ( $D^{\text{mdl}} / D^{\text{w}} \sim 80\%$ ), suggesting some resistance in the ensemble. These results seem to be  
 321 consistent with previous experimental observations with anions [18, 51, 52]. Furthermore, there  
 322 is a significant difference between  $D^{\text{mdl}}$  and  $D^{\text{eff}}$  ( $D^{\text{eff}} / D^{\text{mdl}} \sim 75\%$ ). Consequently,  $M_{\text{th1}}$  does not  
 323 match with  $M_{\text{DGT}}$  as shown with the red dashed line in Figure 3. Investigations were carried out  
 324 to check whether this lower than expected  $M_{\text{DGT}}$  could be the result from a longer diffusion path.  
 325 A thin diffusion-controlled layer, known as diffusive boundary layer (DBL), exists at any solid  
 326 surface in aqueous environment, even in vigorously stirred solutions. The DBL is known to affect  
 327 the DGT results [53, 54]. That is the reason why its thickness ( $\delta^{\text{dbl}}$ ) was assessed by using  
 328 different thickness of diffusive gel in the AgdCl-DGT samplers. Experimental details are  
 329 presented in section S7. A linear plot of the reciprocal mass of  $\Gamma$  versus  $\delta^{\text{mdl}}$  was observed ( $R^2 =$   
 330  $0.998$ ; Figure S8). The slope and the intercept were classically used to calculate  $\delta^{\text{dbl}}$  according to  
 331 Eq. S2. Our  $\delta^{\text{dbl}}$  is  $361 \pm 40 \mu\text{m}$ , indicating that the mixing of deployment solution was not  
 332 optimal. Indeed, common  $\delta^{\text{dbl}}$  values were close to  $200 \mu\text{m}$  in well mixed solution [55]. As  $\delta^{\text{dbl}}$  is  
 333 not negligible, we propose now to include it in calculation of the theoretical mass accumulated of  
 334  $\Gamma$  (Eq. 6):

$$M_{th2} = \frac{C_I \times A_P \times t}{\left( \frac{\delta^{dbl1}}{D^w} + \frac{\delta^{mdl}}{D^{mdl}} \right)} \quad \text{Eq. 6}$$

335 Results are displayed with the orange dashed line in Figure 3. The impact of considering the DBL  
 336 is a decrease of 23.5 % in theoretical accumulation when comparing  $M_{th1}$  and  $M_{th2}$ , but there is  
 337 still some difference with  $M_{DGT}$  points. The reduced slope could indicate that the accumulation of  
 338  $\Gamma$  does not fulfil perfect sink condition *i.e.*, the concentration of  $\Gamma$  in the resin-diffusive gel  
 339 interface is not zero and  $\Gamma$  penetrates into the resin domain [56]. This assumption was tested  
 340 using DGT samplers equipped with a stack of two AgdCl-binding gels in two deployment  
 341 solution containing 1 and 10 mmol L<sup>-1</sup> NaCl (see experiment details in section S8).  $\Gamma$  was present  
 342 at 8.7 and 0.3 % in the back binding gel when AgdCl-DGT samplers were deployed in 1 and 10  
 343 mmol L<sup>-1</sup> NaCl solution, respectively. Knowing the distribution of  $\Gamma$  in the stack of two AgdCl-  
 344 binding gels, it is now possible to determine the penetration factor  $\lambda_M$  *i.e.*, the mean distance that  
 345  $\Gamma$  can penetrate into an AgdCl-binding gel.  $\lambda_M$  is calculated from Eq. S3, and the average value  
 346 obtained is  $312 \pm 100 \mu\text{m}$  and  $140.8 \pm 8.4 \mu\text{m}$  for deployment solution composed of 1 and 10  
 347 mmol L<sup>-1</sup> NaCl, respectively. The AgdCl-resin beads have a size ranging between 40 to 125  $\mu\text{m}$   
 348 (Figure S9). More precisely, the diameter of AgdCl-resin beads defining 10%, 50% and 90% of  
 349 the cumulative volume undersize is 55  $\mu\text{m}$ , 73  $\mu\text{m}$  and 97  $\mu\text{m}$ , respectively. As  $\lambda_M$  is significantly  
 350 higher than the diameter of AgdCl-resin beads, we confirm that the AgdCl-resin does not act as a  
 351 perfect sink and there is a non-null concentration of  $\Gamma$  all along the resin disc. Consequently, for  
 352 this case where there is a resulting kinetic limitation, we propose a new expression to estimate the  
 353 accumulation of DGT samplers (Eq. 7):

$$M_{th3} = \frac{C_I \times A_P \times t}{\left( \frac{\delta^{dbl2}}{D^w} + \frac{\delta^{mdl}}{D^{mdl}} + \frac{\lambda_M \times \coth(\delta^r/\lambda_M)}{\Pi \times D^{gel}} \right)} \quad \text{Eq. 7}$$

354 where  $\delta^r$  correspond to the thickness of AgdCl-binding gel (0.08 cm) and the term  $\lambda_M \times$   
 355  $\coth(\delta^r/\lambda_M)$  to the effective distance of penetration of  $\Gamma$  in the AgdCl-resin domain (cm).  $\Pi$  is  
 356 the ratio between the analyte concentration inside the binding gel disc and the concentration  
 357 inside the diffusive gel disc, both at the limiting interface between the two gel discs [46]. Another  
 358 new equation was used to recalculate the thickness of DBL ( $\delta^{dbl2}$ , cm) taking into account the  
 359 penetration phenomenon and the electrostatic partitioning between the two gel discs:

$$\delta^{dbl2} = D^w \left( \frac{y}{s \times D^{mdl}} - \frac{\lambda_M \times \coth(\delta^r/\lambda_M)}{\Pi \times D^{gel}} \right) \quad \text{Eq. 8}$$

360 An electrostatic correction could be done, but it requires complementary experiments to  
 361 determine  $\Pi$ . As a first approximation, we have taken  $\Pi = 1$  in Eq.7 and Eq. 8. The  $\delta^{dbl2}$  value  
 362 ( $326 \pm 42 \mu\text{m}$ ) is slightly lower than  $\delta^{dbl1}$ . Results are shown with the green dashed line in Figure  
 363 3. The  $M_{th3}$  curve is a better fit to simulate the uptake of  $\Gamma$  by AgdCl-DGT sampler ( $M_{DGT} / M_{th3}$   
 364  $= 98 \pm 8 \%$ ) compared to the  $M_{th1}$  and  $M_{th2}$  curves ( $M_{DGT} / M_{th1} = 71 \pm 6 \%$  and  $M_{DGT} / M_{th2} = 93 \pm$   
 365  $7 \%$ ). Similar results were obtained for the DGT experiment using a stack of two AgdCl in 10  
 366  $\text{mmol L}^{-1}$  NaCl ( $M_{DGT} / M_{th3} = 106 \pm 6 \%$ ). Eq. 7 will be used to evaluate the AgdCl-DGT  
 367 performances in the following sections. Nevertheless, application of Eq. 7 (with  $\Pi = 1$ ) does not  
 368 explain the low amount of  $\Gamma$  found in the two AgdCl-binding gels for the DGT experiment  
 369 performed in 1  $\text{mmol L}^{-1}$  NaCl ( $M_{DGT} / M_{th3} = 4.1 \pm 0.3 \%$ ). The low DGT response is probably  
 370 linked to the partial exclusion of anions from the resin at low ionic strength, which would be  
 371 quantified by the parameter  $\Pi$ . This exclusion from the AgdCl-resin seems more likely than  
 372 exclusion from the filter and diffusive gel as previously observed in previous laboratory  
 373 validation of DGT methods [43, 48]. Additional experiments will focus on the effect of ionic  
 374 strength in section 3.2.6.

375 Complementary, DGT experiments were done to control the possibility of using the AgdCl-  
376 binding gel for redox speciation. For this experiment,  $\text{IO}_3^-$  and  $\Gamma$  were simultaneously present in  
377 deployment solution with different weight ratio  $[\Gamma] / [\text{IO}_3^-]$  up to 4.6 (Figure 4). To confirm the  
378 selectivity of AgdCl-DGT method for  $\Gamma$ ,  $M_{\text{th}3}$  was calculated using the concentration of  $\Gamma$   
379 measured by IC-ICP-MS (Eq. 7). Acceptable DGT measurements were obtained for  $M_{\text{DGT}} / M_{\text{th}3}$   
380  $= 100 \pm 15 \%$  (dashed lines in Figure 4), as in other previous DGT laboratory evaluations [19, 20,  
381 39]. Whatever the weight ratio  $[\Gamma] / [\text{IO}_3^-]$  tested, the AgdCl-DGT estimations were good with  
382  $M_{\text{DGT}} / M_{\text{th}3}$  values ranging between 89 and 107 %. As the DGT measurements were not  
383 interfered by  $\text{IO}_3^-$ , it is confirmed that the AgdCl-binding gel is only selective to  $\Gamma$ .

### 384 3.2.3. Effect of pH

385 The impact of pH on the accumulation of  $\Gamma$  was investigated for 10 h of deployment time. Over  
386 the pH range from 4.5 to 8.8, excellent agreement was observed between the predicted and  
387 accumulated mass of  $\Gamma$  ( $M_{\text{DGT}} / M_{\text{th}3} = 93 - 113 \%$ ; Figure S10). These results indicate that the  
388 performance of the AgdCl-DGT method is independent of pH over the typical range found in  
389 environmental waters (pH  $\sim$  5-9).

### 390 3.2.4. AgdCl-DGT sampler binding capacity

391 To determine the AgdCl-DGT sampler binding capacity to accumulate  $\Gamma$ , a time-series  
392 experiment was performed using a high concentration of this species ( $\sim 20 \text{ mg L}^{-1}$ ) in deployment  
393 solution with  $[\text{NaCl}] = 10 \text{ mmol L}^{-1}$  and pH = 5.5. Linear accumulation of  $\Gamma$  by AgdCl-DGT  
394 samplers was observed up to 6 h ( $R^2 > 0.95$ ; Figure S11). The AgdCl-DGT response was in  
395 agreement with predicted total  $\Gamma$  mass since the  $M_{\text{DGT}} / M_{\text{th}3}$  value was  $106 \pm 7 \%$  (mean  $\pm$   
396 standard deviation). After 8 h of deployment time, the  $M_{\text{DGT}}$  values decreased compared with  
397  $M_{\text{th}3}$  values. The maximum mass of  $\Gamma$  accumulated by AgdCl-DGT samplers was  $218 \pm 25 \mu\text{g}$ . As



398 inorganic I species occur at trace levels in environmental waters ( $< 100 \mu\text{g L}^{-1}$ ), this binding  
399 capacity should be high enough to deploy AgdCl-DGT samplers during 24 - 96 h (typical  
400 deployment times).

### 401 **3.2.5. Effect of bicarbonates**

402 The effect of  $\text{HCO}_3^-$  on the accumulation was investigated up to 24 h.  $M_{\text{DGT}}$  agrees with  $M_{\text{th3}}$   
403 within an error of 15 % (Figure S12;  $105 \pm 5$  and  $104 \pm 7$  % for 1 and 5  $\text{mmol L}^{-1}$   $\text{HCO}_3^-$ ,  
404 respectively). In these conditions,  $\text{HCO}_3^-$  is not a competing ion for the accumulation of  $\text{I}^-$  by  
405 AgdCl-DGT samplers. That is consistent with thermodynamic data. Indeed, the precipitation of  
406  $\text{Ag}_2\text{CO}_3$  does not hinder AgI formation when comparing solubility product constant values ( $\text{pK}_{\text{sp}}$   
407 = 11.1 and 16.1 for  $\text{Ag}_2\text{CO}_3$  and AgI, respectively [41]).

### 408 **3.2.6. Time-series experiment in natural and synthetic waters**

409 After carrying out numerous experiments in 10  $\text{mmol L}^{-1}$  NaCl solutions, the performances of  
410 AgdCl-DGT method were studied in Vittel® and Volvic® water spiked with  $\text{I}^-$  with a  
411 concentration close to 20  $\mu\text{g L}^{-1}$ . The concentration of  $\text{IO}_3^-$  was negligible in these deployment  
412 solutions with values lower than 1  $\mu\text{g L}^{-1}$ . The ionic strength for these two drinking waters are  
413 22.6 and 3.2  $\text{mmol L}^{-1}$ , respectively (calculations performed by using data in Table 1 and  
414 PHREEQC software). The mass of  $\text{I}^-$  accumulated by AgdCl-DGT samplers was monitored over  
415 time, and compared to  $M_{\text{th3}}$  (black line in Figure 5). Linear accumulation of total I mass by  
416 AgdCl-DGT samplers was observed up to 24 h for Vittel® and Volvic® waters ( $R^2 > 0.9$ ; Figure  
417 5 (A) and (B)). However, the amount of  $\text{I}^-$  measured by AgdCl-DGT samplers was  $33 \pm 8$  and  $27$   
418  $\pm 5$  % in Vittel® and Volvic® waters, respectively. Assuming 15 % of error on predicted total I  
419 mass (dashed lines in Figure 5), the AgdCl-DGT measurements were not quantitative whatever  
420 the deployment times. Although the ionic strength of these two drinking waters was significantly

421 different, similar DGT responses were obtained. It is also noted that Vittel® water had a higher  
422 ionic strength than the synthetic deployment solution employed to characterize the AgdCl-DGT  
423 performances, but the pH was much higher in the natural waters. Possibly, AgdCl-resin has acid-  
424 base properties (data not found in the literature). If pH overcomes the pKa of the AgdCl-resin, the  
425 amount of negative charge sites in the AgdCl-resin might increase remarkably. More charge  
426 means more electrostatic potential, more exclusion of anions from the resin and less  
427 accumulation. This speculation is not however fully consistent with the pH-impact figure (Figure  
428 S10).

429 New time-series experiments were performed to verify whether the AgdCl-DGT method depends  
430 on the concentration of  $\text{Cl}^-$ . Vittel® and Volvic® water were consequently spiked with ultrapure  
431 NaCl salt to reach a concentration of  $\text{Cl}^-$  at  $10 \text{ mmol L}^{-1}$  (value used in previous experiments  
432 using synthetic waters). The ionic strength values are  $32.9$  and  $13 \text{ mmol L}^{-1}$  for NaCl-doped  
433 Vittel® and Volvic® water, respectively. When AgdCl-DGT samplers are deployed in the two  
434 NaCl-doped drinking waters, better DGT responses were obtained compared with non-spiked  
435 drinking waters (Figure 5 (C) and (D)). Indeed, the amount of total mass of  $\Gamma$  measured by  
436 AgdCl-DGT samplers were  $77 \pm 4$  and  $72 \pm 4$  % in NaCl-doped Vittel® and Volvic® waters,  
437 respectively. The presence of  $\text{SO}_4^{2-}$  was then tested only with Volvic® water spiked with  
438 ultrapure  $\text{Na}_2\text{SO}_4$  salt to a concentration of  $\text{SO}_4^{2-}$  at  $10 \text{ mmol L}^{-1}$ . This time, the amount of  $\Gamma$   
439 measured by AgdCl-DGT samplers reached  $107 \pm 3$  % (Figure 5 (E)). This means an increase of  
440 the AgdCl-DGT response with anions another than  $\text{Cl}^-$  and supports the key role of ionic strength.

441 Although the direct application of AgdCl-DGT method will not be possible in continental waters,  
442 the deployment of AgdCl-DGT samplers could be envisaged in seawater and brine due to high  
443 concentration of  $\text{Cl}^-$  and  $\text{SO}_4^{2-}$ . To confirm the latter hypothesis, a time-series experiment was

444 performed in synthetic seawater spiked with  $\Gamma$  concentration close to  $100 \mu\text{g L}^{-1}$ . Long  
445 deployment times were used to reveal possible interferences of AgdCl-binding gel. As shown in  
446 Figure 5 (F), linear accumulation of  $\Gamma$  by AgdCl-DGT samplers was observed up to 72 h ( $R^2 >$   
447  $0.95$ ). The mass of  $\Gamma$  recovered by the AgdCl-DGT samplers reached  $107 \pm 5 \%$ , validating the  
448 suitability of the AgdCl-DGT method for application in seawater. The AgdCl-DGT method  
449 allowed to concentrate  $\Gamma$  by a factor 24 ( $C_e / C_D$ ), which is useful to measure low  $\Gamma$   
450 concentrations. Furthermore, the saturation of AgdCl-binding gel was not experimentally  
451 observed in this long time-series experiment. This result also confirms that there is no  
452 interference with  $\text{HCO}_3^-$  ( $2.38 \text{ mmol L}^{-1}$ ).

#### 453 **4. Conclusions**

454 The DGT performances of AgdCl-DGT binding gel to measure the concentration of at least one  
455 inorganic I species have been tested. A rigorous experimental design involving batch and time-  
456 series experiments was performed in order to gain knowledge on AgdCl-binding gel selectivity  
457 and limitations as well as to establish a robust DGT deployment protocol. This works shows that  
458 the AgdCl-DGT sampler is able to accumulate selectively  $\Gamma$ . The AgdCl-DGT response is not pH  
459 dependent (4.5 -8.8). The quantification of  $\Gamma$  concentration is not impacted by the presence of  
460  $\text{IO}_3^-$  and  $\text{HCO}_3^-$ . Nevertheless, the current AgdCl-DGT method requires high ionic strength in  
461 deployment solution limiting the application of to sea or brine waters. Further work should  
462 investigate the possibility of analyzing freshwaters using an effective diffusion coefficient  
463 determined at the same pH and ionic strength as the one of the natural sample.

464 This analytical development validates a first step to perform redox speciation for I using DGT  
465 techniques, and other developments could be performed to find a binding gel only able to  
466 accumulate  $\text{IO}_3^-$  or the two inorganic I species simultaneously. To avoid the harmful

467 manipulation of KCN eluent solution, laboratory equipped with pyrolyser could develop  
468 alternative extraction strategies by trapping the gaseous iodine from AgdCl binding in alkaline  
469 solution (TMAH, NaOH-NaHSO<sub>3</sub>) [57-61]. Finally, future research should focus on the  
470 application of the AgdCl-DGT method to study the biochemistry of iodide in marine or brine  
471 environments, but also to better predict the <sup>129</sup>I behavior from spent nuclear fuel reprocessing  
472 plants.

### 473 **Acknowledgements**

474 This work has been supported by the ANR (French National Research Agency), under the  
475 “Investissement d’Avenir” framework program [Number ANR-11-RSNR-0002]. Véronique  
476 Hénin (Metrohm France) is gratefully thanked for the loan of the Metrosep Asupp 10 guard and  
477 analytical columns, but also Gilles Alcalde for the granulometric measurements of AgdCl-resin  
478 beads. All experiments were performed at LUTECE (the SEDRE’s experimental platform), and  
479 elemental and speciation measurements at PATERSON (the IRSN’s mass spectrometry  
480 platform). This is PATERSON contribution n°9. Support from the Spanish Ministry of Science  
481 and Innovation is gratefully acknowledged (Project PID2019-107033GB-C21).

482

483 **References**

- 484 [1] R.D. Scheele, L. Burger, C. Matsuzaki, Methyl iodide sorption by reduced silver mordenite,  
485 Pacific Northwest Lab., Richland, WA (USA), 1983.
- 486 [2] X. Hou, V. Hansen, A. Aldahan, G. Possnert, O.C. Lind, G. Lujanene, A review on  
487 speciation of iodine-129 in the environmental and biological samples, *Analytica Chimica Acta*,  
488 632 (2009) 181-196.
- 489 [3] K. Tagami, S. Uchida, Concentrations of chlorine, bromine and iodine in Japanese rivers,  
490 *Chemosphere*, 65 (2006) 2358-2365.
- 491 [4] Y. Takaku, T. Shimamura, K. Masuda, Y. Igarashi, Iodine Determination in Natural and Tap  
492 Water Using Inductively Coupled Plasma Mass Spectrometry, *Analytical Sciences*, 11 (1995)  
493 823-827.
- 494 [5] J. Zheng, H. Takata, K. Tagami, T. Aono, K. Fujita, S. Uchida, Rapid determination of total  
495 iodine in Japanese coastal seawater using SF-ICP-MS, *Microchemical Journal*, 100 (2012) 42-47.
- 496 [6] J.E. Moran, S.D. Oktay, P.H. Santschi, Sources of iodine and iodine 129 in rivers, *Water*  
497 *resources research*, 38 (2002).
- 498 [7] V.W. Truesdalea, S.D. Jones, The variation of iodate and total iodine in some UK rainwaters  
499 during 1980–1981, *Journal of Hydrology*, 179 (1996) 67-86.
- 500 [8] D.C. Whitehead, The distribution and transformations of iodine in the environment,  
501 *Environment International*, 10 (1984) 321-339.
- 502 [9] G.W. Luther, H. Cole, Iodine speciation in chesapeake bay waters, *Marine Chemistry*, 24  
503 (1988) 315-325.
- 504 [10] R.C. Tian, E. Nicolas, Iodine speciation in the northwestern Mediterranean Sea, method and  
505 vertical profile, *Marine Chemistry*, 48 (1995) 151-156.
- 506 [11] B.S. Gilfedder, M. Petri, H. Biester, Iodine speciation and cycling in fresh waters: a case  
507 study from a humic rich headwater lake (Mummelsee), *Journal of Limnology*, 68 (2009) 396-  
508 408.
- 509 [12] S. Zhang, Y.-F. Ho, D. Creeley, K.A. Roberts, C. Xu, H.-P. Li, K.A. Schwehr, D.I. Kaplan,  
510 C.M. Yeager, P.H. Santschi, Temporal variation of Iodine concentration and speciation (127I and  
511 129I) in wetland groundwater from the Savannah River Site, USA, *Environmental science &*  
512 *technology*, 48 (2014) 11218-11226.
- 513 [13] H. Kennedy, H. Elderfield, Iodine diagenesis in pelagic deep-sea sediments, *Geochimica et*  
514 *Cosmochimica Acta*, 51 (1987) 2489-2504.
- 515 [14] H.A. Kennedy, H. Elderfield, Iodine diagenesis in non-pelagic deep-sea sediments,  
516 *Geochimica et Cosmochimica Acta*, 51 (1987) 2505-2514.
- 517 [15] W.J. Ullman, R.C. Aller, Rates of iodine remineralization in terrigenous near-shore  
518 sediments, *Geochimica et Cosmochimica Acta*, 47 (1983) 1423-1432.
- 519 [16] W. Davison, H. Zhang, G.W. Grime, Performance Characteristics of Gel Probes Used For  
520 Measuring the Chemistry of Pore Waters, *Environmental science & technology*, 28 (1994) 1623-  
521 1632.
- 522 [17] H. Zhang, W. Davison, Performance Characteristics of Diffusion Gradients in Thin Films for  
523 the in Situ Measurement of Trace Metals in Aqueous Solution, *Analytical chemistry*, 67 (1995)  
524 3391-3400.
- 525 [18] W.W. Bennett, P.R. Teasdale, J.G. Panther, D.T. Welsh, D.F. Jolley, Speciation of dissolved  
526 inorganic arsenic by diffusive gradients in thin films: selective binding of AsIII by 3-  
527 mercaptopropyl-functionalized silica gel, *Analytical chemistry*, 83 (2011) 8293-8299.

- 528 [19] J. Gorny, L. Lesven, G. Billon, D. Dumoulin, C. Noiriel, C. Pirovano, B. Madé,  
529 Determination of total arsenic using a novel Zn-ferrite binding gel for DGT techniques:  
530 Application to the redox speciation of arsenic in river sediments, *Talanta*, 144 (2015) 890-898.
- 531 [20] J. Gorny, D. Dumoulin, V. Alaimo, L. Lesven, C. Noiriel, B. Madé, G. Billon, Passive  
532 sampler measurements of inorganic arsenic species in environmental waters: A comparison  
533 between 3-mercaptop-silica, ferrihydrite, Metsorb®, zinc ferrite, and zirconium dioxide binding  
534 gels, *Talanta*, 198 (2019) 518-526.
- 535 [21] T.D.W. Corbett, A. Hartland, W. Henderson, G.J. Rys, L.A. Schipper, Development of  
536 Bromide-Selective Diffusive Gradients in Thin-Films for the Measurement of Average Flow Rate  
537 of Streams, *Science of The Total Environment*, (2021) 147737.
- 538 [22] D. Devillers, R. Buzier, S. Simon, A. Charriau, G. Guibaud, Simultaneous measurement of  
539 Cr(III) and Cr(VI) in freshwaters with a single Diffusive Gradients in Thin Films device, *Talanta*,  
540 154 (2016) 533-538.
- 541 [23] Y. Yao, C. Wang, P. Wang, L. Miao, J. Hou, T. Wang, C. Liu, Zr oxide-based coloration  
542 technique for two-dimensional imaging of labile Cr(VI) using diffusive gradients in thin films,  
543 *Science of The Total Environment*, 566–567 (2016) 1632-1639.
- 544 [24] H. Chen, Y.-Y. Zhang, K.-L. Zhong, L.-W. Guo, J.-L. Gu, L. Bo, M.-H. Zhang, J.-R. Li,  
545 Selective sampling and measurement of Cr (VI) in water with polyquaternary ammonium salt as  
546 a binding agent in diffusive gradients in thin-films technique, *Journal of Hazardous Materials*,  
547 271 (2014) 160-165.
- 548 [25] Y. Gao, E. De Canck, M. Leermakers, W. Baeyens, P. Van Der Voort, Synthesized  
549 mercaptopropyl nanoporous resins in DGT probes for determining dissolved mercury  
550 concentrations, *Talanta*, 87 (2011) 262-267.
- 551 [26] O. Clarisse, D. Foucher, H. Hintelmann, Methylmercury speciation in the dissolved phase of  
552 a stratified lake using the diffusive gradient in thin film technique, *Environmental Pollution*, 157  
553 (2009) 987-993.
- 554 [27] J. Huang, W.W. Bennett, P.R. Teasdale, N.R. Kankanamge, D.T. Welsh, A modified DGT  
555 technique for the simultaneous measurement of dissolved inorganic nitrogen and phosphorus in  
556 freshwaters, *Analytica Chimica Acta*, 988 (2017) 17-26.
- 557 [28] M. Ren, S. Ding, D. Shi, Z. Zhong, J. Cao, L. Yang, D.C.W. Tsang, D. Wang, D. Zhao, Y.  
558 Wang, A new DGT technique comprised in a hybrid sensor for the simultaneous measurement of  
559 ammonium, nitrate, phosphorus and dissolved oxygen, *Science of The Total Environment*, 725  
560 (2020) 138447.
- 561 [29] J. Huang, W.W. Bennett, D.T. Welsh, P.R. Teasdale, Determining time-weighted average  
562 concentrations of nitrate and ammonium in freshwaters using DGT with ion exchange  
563 membrane-based binding layers, *Environmental Science: Processes & Impacts*, 18 (2016) 1530-  
564 1539.
- 565 [30] C. Han, P.N. Williams, J. Ren, Z. Wang, X. Fang, D. Xu, X. Xie, J. Geng, L.Q. Ma, J. Luo,  
566 In situ sampling and speciation method for measuring dissolved phosphite at ultratrace  
567 concentrations in the natural environment, *Water Research*, 137 (2018) 281-289.
- 568 [31] P.R. Teasdale, S. Hayward, W. Davison, In situ, High-Resolution Measurement of Dissolved  
569 Sulfide Using Diffusive Gradients in Thin Films with Computer-Imaging Densitometry,  
570 *Analytical chemistry*, 71 (1999) 2186-2191.
- 571 [32] O. Hanousek, S. Mason, J. Santner, M.M.A. Chowdhury, T.W. Berger, T. Prohaska, Novel  
572 diffusive gradients in thin films technique to assess labile sulfate in soil, *Analytical and*  
573 *Bioanalytical Chemistry*, 408 (2016) 6759-6767.

- 574 [33] W. Bennett, M. Arsic, D.T. Welsh, P. Teasdale, In situ speciation of dissolved inorganic  
575 antimony in surface waters and sediment porewaters: development of a thiol-based diffusive  
576 gradients in thin films technique for Sb III, *Environmental Science: Processes & Impacts*, (2016).
- 577 [34] H.-T. Fan, A.-J. Liu, B. Jiang, Q.-J. Wang, T. Li, C.-C. Huang, Sampling of dissolved  
578 inorganic SbIII by mercapto-functionalized silica-based diffusive gradients in thin-film  
579 technique, *RSC Advances*, 6 (2016) 2624-2631.
- 580 [35] H.L. Price, P.R. Teasdale, D.F. Jolley, An evaluation of ferrihydrite- and Metsorb™-DGT  
581 techniques for measuring oxyanion species (As, Se, V, P): Effective capacity, competition and  
582 diffusion coefficients, *Analytica Chimica Acta*, 803 (2013) 56-65.
- 583 [36] K.S. Luko, A.A. Menegário, C.A. Suárez, M. Tafurt-Cardona, J.H. Pedrobon, A.M.C.M.  
584 Rolisola, E.T. Sulato, C.H. Kiang, In situ determination of V(V) by diffusive gradients in thin  
585 films and inductively coupled plasma mass spectrometry techniques using amberlite IRA-410  
586 resin as a binding layer, *Analytica Chimica Acta*, 950 (2017) 32-40.
- 587 [37] A. Zulauf, S. Happel, M.B. Mokili, A. Bombard, H. Jungclas, Characterization of an  
588 extraction chromatographic resin for the separation and determination of <sup>36</sup>Cl and <sup>129</sup>I, *Journal*  
589 *of Radioanalytical and Nuclear Chemistry*, 286 (2010) 539-546.
- 590 [38] C. Decamp, S. Happel, Utilization of a mixed-bed column for the removal of iodine from  
591 radioactive process waste solutions, *Journal of Radioanalytical and Nuclear Chemistry*, 298  
592 (2013) 763-767.
- 593 [39] J. Gorny, A. Gourgiotis, F. Coppin, L. Février, H. Zhang, C. Simonucci, Better  
594 understanding and applications of ammonium 12-molybdophosphate-based diffusive gradient in  
595 thin film techniques for measuring Cs in waters, *Environmental Science and Pollution Research*,  
596 26 (2019) 1994-2006.
- 597 [40] H. Zhang, W. Davison, Diffusional characteristics of hydrogels used in DGT and DET  
598 techniques, *Analytica Chimica Acta*, 398 (1999) 329-340.
- 599 [41] G. Charlot, *Les réactions chimiques en solution et caractérisation des ions*, 7th ed.1983.
- 600 [42] H. Dočekalová, P. Diviš, Application of diffusive gradient in thin films technique (DGT) to  
601 measurement of mercury in aquatic systems, *Talanta*, 65 (2005) 1174-1178.
- 602 [43] Y. Wang, S. Ding, M. Gong, S. Xu, W. Xu, C. Zhang, Diffusion characteristics of agarose  
603 hydrogel used in diffusive gradients in thin films for measurements of cations and anions,  
604 *Analytica Chimica Acta*, 945 (2016) 47-56.
- 605 [44] P. Diviš, R. Szkandera, H. Dočekalová, Characterization of sorption gels used for  
606 determination of mercury in aquatic environment by diffusive gradients in thin films technique,  
607 *Central European Journal of Chemistry*, 8 (2010) 1105-1109.
- 608 [45] S. Mongin, R. Uribe, J. Puy, J. Cecilia, J. Galceran, H. Zhang, W. Davison, Key Role of the  
609 Resin Layer Thickness in the Lability of Complexes Measured by DGT, *Environmental science*  
610 *& technology*, 45 (2011) 4869-4875.
- 611 [46] J. Puy, J. Galceran, S. Cruz-González, C.A. David, R. Uribe, C. Lin, H. Zhang, W. Davison,  
612 Measurement of Metals Using DGT: Impact of Ionic Strength and Kinetics of Dissociation of  
613 Complexes in the Resin Domain, *Analytical chemistry*, 86 (2014) 7740-7748.
- 614 [47] J. Galceran, J. Puy, Interpretation of diffusion gradients in thin films (DGT) measurements:  
615 a systematic approach, *Environmental Chemistry*, 12 (2015) 112-122.
- 616 [48] A.-L. Pommier, R. Buzier, S. Simon, G. Guibaud, Impact of low ionic strength on DGT  
617 sampling with standard APA gels: Effect of pH and analyte, *Talanta*, 222 (2021) 121413.
- 618 [49] E. Giffaut, M. Grivé, P. Blanc, P. Vieillard, E. Colàs, H. Gailhanou, S. Gaboreau, N. Marty,  
619 B. Madé, L. Duro, Andra thermodynamic database for performance assessment: ThermoChimie,  
620 *Applied Geochemistry*, 49 (2014) 225-236.

- 621 [50] D.L. Parkhurst, C. Appelo, Description of input and examples for PHREEQC version 3: a  
622 computer program for speciation, batch-reaction, one-dimensional transport, and inverse  
623 geochemical calculations, US Geological Survey, 2013.
- 624 [51] H. Zhang, W. Davison, R. Gadi, T. Kobayashi, In situ measurement of dissolved phosphorus  
625 in natural waters using DGT, *Analytica Chimica Acta*, 370 (1998) 29-38.
- 626 [52] J.G. Panther, R.R. Stewart, P.R. Teasdale, W.W. Bennett, D.T. Welsh, H. Zhao, Titanium  
627 dioxide-based DGT for measuring dissolved As(V), V(V), Sb(V), Mo(VI) and W(VI) in water,  
628 *Talanta*, 105 (2013) 80-86.
- 629 [53] Ø.A. Garmo, K.R. Naqvi, O. Røyset, E. Steinnes, Estimation of diffusive boundary layer  
630 thickness in studies involving diffusive gradients in thin films (DGT), *Analytical and*  
631 *Bioanalytical Chemistry*, 386 (2006) 2233-2237.
- 632 [54] K.W. Warnken, H. Zhang, W. Davison, Accuracy of the Diffusive Gradients in Thin-Films  
633 Technique: Diffusive Boundary Layer and Effective Sampling Area Considerations, *Analytical*  
634 *chemistry*, 78 (2006) 3780-3787.
- 635 [55] W. Davison, H. Zhang, Progress in understanding the use of diffusive gradients in thin films  
636 (DGT)–back to basics, *Environmental Chemistry*, 9 (2012) 1-13.
- 637 [56] J.L. Levy, H. Zhang, W. Davison, J. Puy, J. Galceran, Assessment of trace metal binding  
638 kinetics in the resin phase of diffusive gradients in thin films, *Analytica Chimica Acta*, 717  
639 (2012) 143-150.
- 640 [57] X. Hou, Y. Wang, Determination of ultra-low level <sup>129</sup>I in vegetation using pyrolysis for  
641 iodine separation and accelerator mass spectrometry measurements, *Journal of Analytical Atomic*  
642 *Spectrometry*, 31 (2016) 1298-1310.
- 643 [58] T. Ohno, Y. Muramatsu, Y. Shikamori, C. Toyama, N. Okabe, H. Matsuzaki, Determination  
644 of ultratrace <sup>129</sup>I in soil samples by Triple Quadrupole ICP-MS and its application to Fukushima  
645 soil samples, *Journal of Analytical Atomic Spectrometry*, 28 (2013) 1283-1287.
- 646 [59] Y. Muramatsu, Y. Ohmomo, M. Sumiya, Determination of iodine-129 and iodine-127 in  
647 environmental samples collected in Japan, *Journal of Radioanalytical and Nuclear Chemistry*,  
648 123 (1988) 181-189.
- 649 [60] E. Englund, A. Aldahan, G. Possnert, V. Alfimov, A routine preparation method for AMS  
650 measurement of <sup>129</sup>I in solid material, *Nuclear Instruments and Methods in Physics Research*  
651 *Section B: Beam Interactions with Materials and Atoms*, 259 (2007) 365-369.
- 652 [61] L. Zhang, W. Zhou, X. Hou, N. Chen, Q. Liu, C. He, Y. Fan, M. Luo, Z. Wang, Y. Fu, Level  
653 and source of <sup>129</sup>I of environmental samples in Xi'an region, China, *Science of The Total*  
654 *Environment*, 409 (2011) 3780-3788.
- 655 [62] K. Grasshoff, K. Kremling, M. Ehrhardt, *Methods of seawater analysis*, John Wiley &  
656 *Sons*2009.
- 657 [63] D.R. Lide, *CRC handbook of chemistry and physics*, CRC press2004.

658

659

660



661 **Figure caption**

662 Figure 1: Uptake factor of inorganic I species by AgdCl-binding gel as a function of: (A) NaCl  
 663 concentration for 24 h of immersion time; (B) Na<sub>2</sub>SO<sub>4</sub> concentration for 24 h of immersion time;  
 664 and (C) immersion time-series in an immersion solution containing either 10 mmol L<sup>-1</sup> NaCl or  
 665 Na<sub>2</sub>SO<sub>4</sub>. Experimental conditions: 20 mL of immersion solution; [NaCl] or [Na<sub>2</sub>SO<sub>4</sub>] = 1-500  
 666 mmol L<sup>-1</sup>; [IO<sub>3</sub><sup>-</sup>] or [I<sup>-</sup>] ~ 100 µg L<sup>-1</sup>; pH = 5.5 ± 0.1.

667 Figure 2: Recovery of I<sup>-</sup> species in the presence of AgdCl-binding gel as a function of KCN  
 668 concentration. Black dashed line corresponds to the minimum acceptable recovery of I<sup>-</sup> (75 %).  
 669 Experimental conditions: 3 mL of eluent solution; [KCN] = 0.1-100 mmol L<sup>-1</sup>; [I<sup>-</sup>] ~ 100 µg L<sup>-1</sup>;  
 670 24 h of immersion.

671 Figure 3: Evolution of the mass of IO<sub>3</sub><sup>-</sup> or I<sup>-</sup> accumulated by AgdCl-DGT samplers over time.  
 672 Dashed lines correspond to the DGT response simulations using Eq. 4, Eq.6 and Eq. 7 for  $M_{th1}$ ,  
 673  $M_{th2}$  and  $M_{th3}$ , respectively. Experimental conditions: 8 L of deployment solution; [NaCl] = 10  
 674 mmol L<sup>-1</sup>; [IO<sub>3</sub><sup>-</sup>] or [I<sup>-</sup>] ~ 30 µg L<sup>-1</sup>; pH = 5.5 ± 0.1;  $T = 20.7 \pm 1.0^\circ\text{C}$ ; up to 10 h of deployment  
 675 time.

676 Figure 4: Confirmation of the selectivity of AgdCl-DGT samplers for inorganic I species. Black  
 677 dashed lines correspond to ± 15 % acceptable error on the DGT measurement. Experimental  
 678 conditions: 8 L of deployment solution; [NaCl] = 10 mmol L<sup>-1</sup>; weight ratio  
 679 [I<sup>-</sup>]/[IO<sub>3</sub><sup>-</sup>] = 0-4.6 obtained by IC-ICP-MS; [IO<sub>3</sub><sup>-</sup>] ~ 20 µg L<sup>-1</sup>; pH = 5.5 ± 0.1; 10 h of deployment  
 680 time.

681 Figure 5: Results of time-series experiments performed with (A) Vittel® water ([I<sup>-</sup>] = 31.6 ± 0.6  
 682 µg L<sup>-1</sup>;  $T = 20.5 \pm 1.1$ ; pH = 8.3 ± 0.2), (B) Volvic® water ([I<sup>-</sup>] = 24.0 ± 0.4 µg L<sup>-1</sup>;  $T = 20.5 \pm$

683 1.1; pH =  $8.0 \pm 0.2$ ), (C) Vittel® water with 10 mmol L<sup>-1</sup> NaCl salt addition ([I] =  $24.7 \pm 1.1$  µg  
684 L<sup>-1</sup>; T =  $20.5 \pm 1.1$  °C; pH =  $8.3 \pm 0.2$ ); (D) Volvic® water with 10 mmol L<sup>-1</sup> NaCl salt addition  
685 ([I] =  $26.3 \pm 1.2$ ; pH =  $8.1 \pm 0.2$ ; T =  $20.5 \pm 1.1$  °C); (E) Volvic® water with 10 mmol L<sup>-1</sup>  
686 Na<sub>2</sub>SO<sub>4</sub> salt addition ([I] =  $16.7 \pm 0.9$ ; pH =  $8.0 \pm 0.2$ ; T =  $20.4 \pm 0.4$  °C); and (F) synthetic  
687 seawater ([I] =  $103.8 \pm 1.2$ ; T =  $20.9 \pm 0.3$  °C; pH =  $8.2 \pm 0.1$ ). The concentration of IO<sub>3</sub><sup>-</sup> was  
688 still lower than 1 µg L<sup>-1</sup> in each deployment solution. Lines for theoretical prediction as in Figure  
689 4.

690

Figure 1

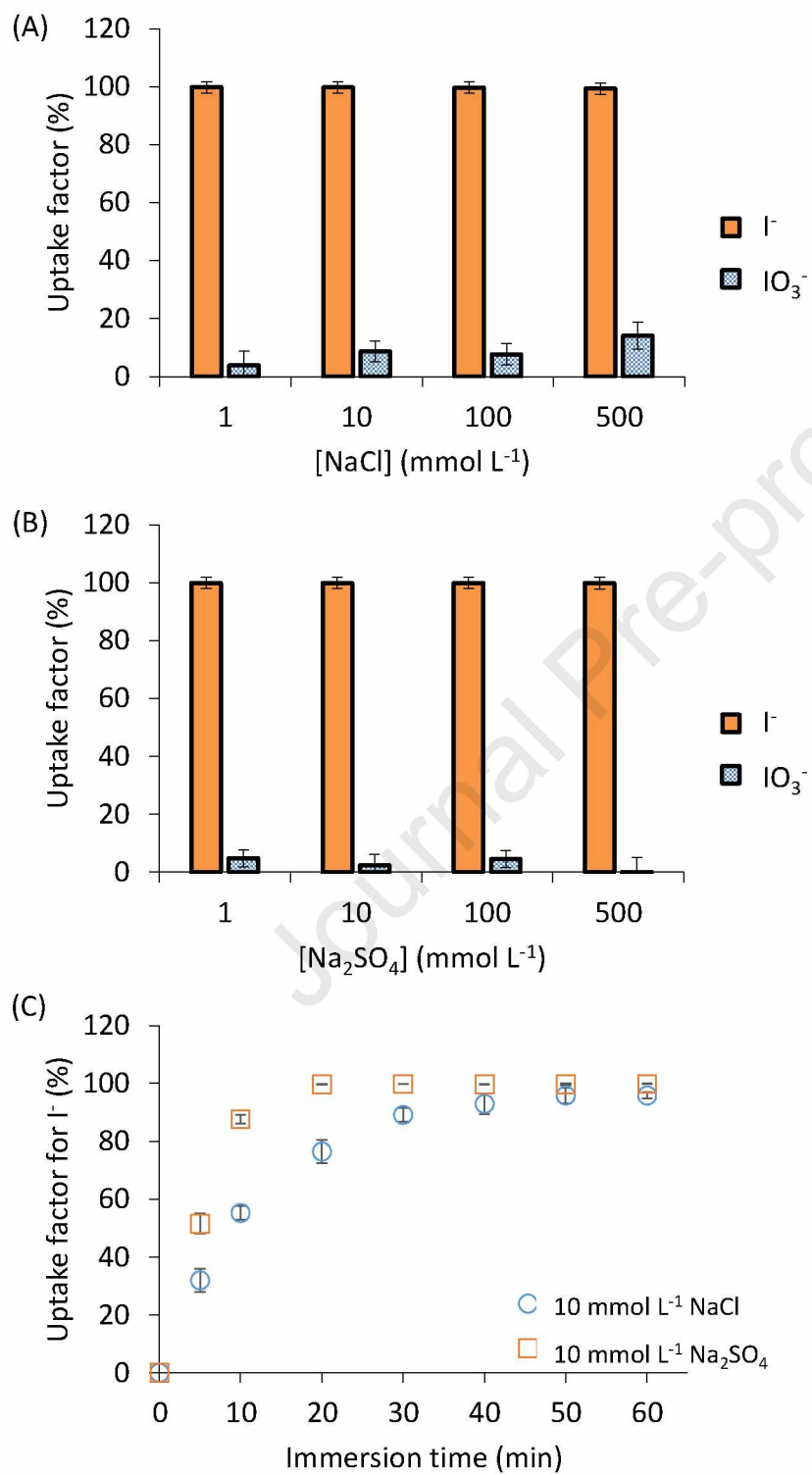


Figure 2

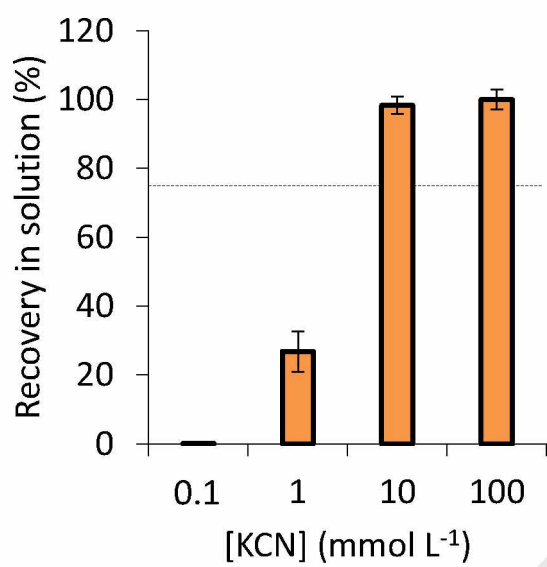


Figure 3

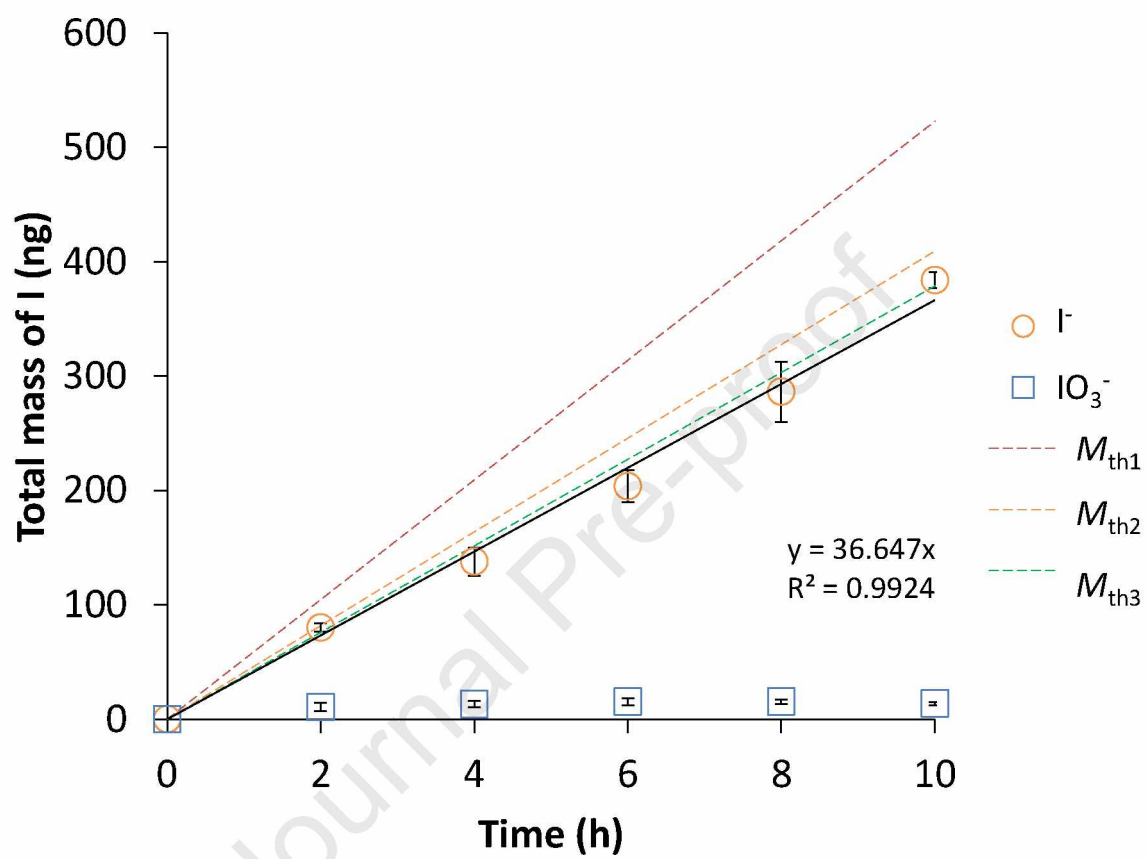


Figure 4

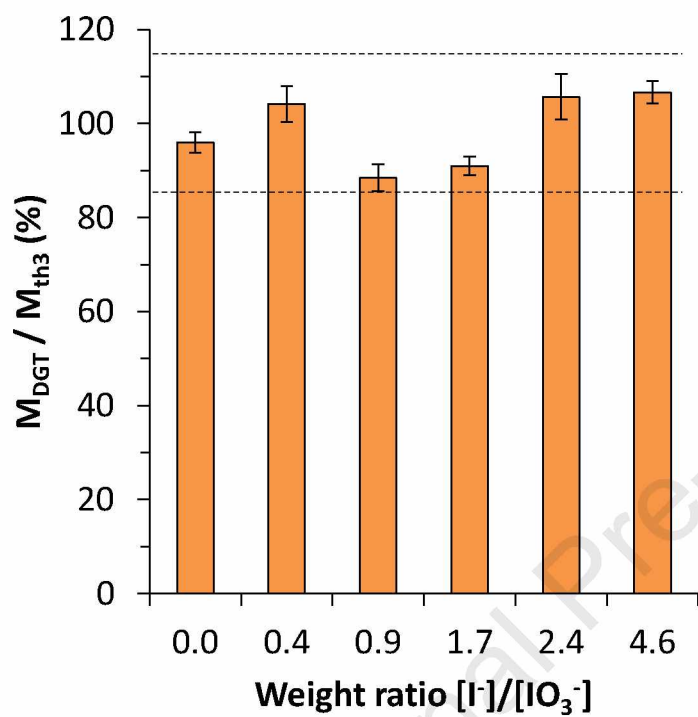
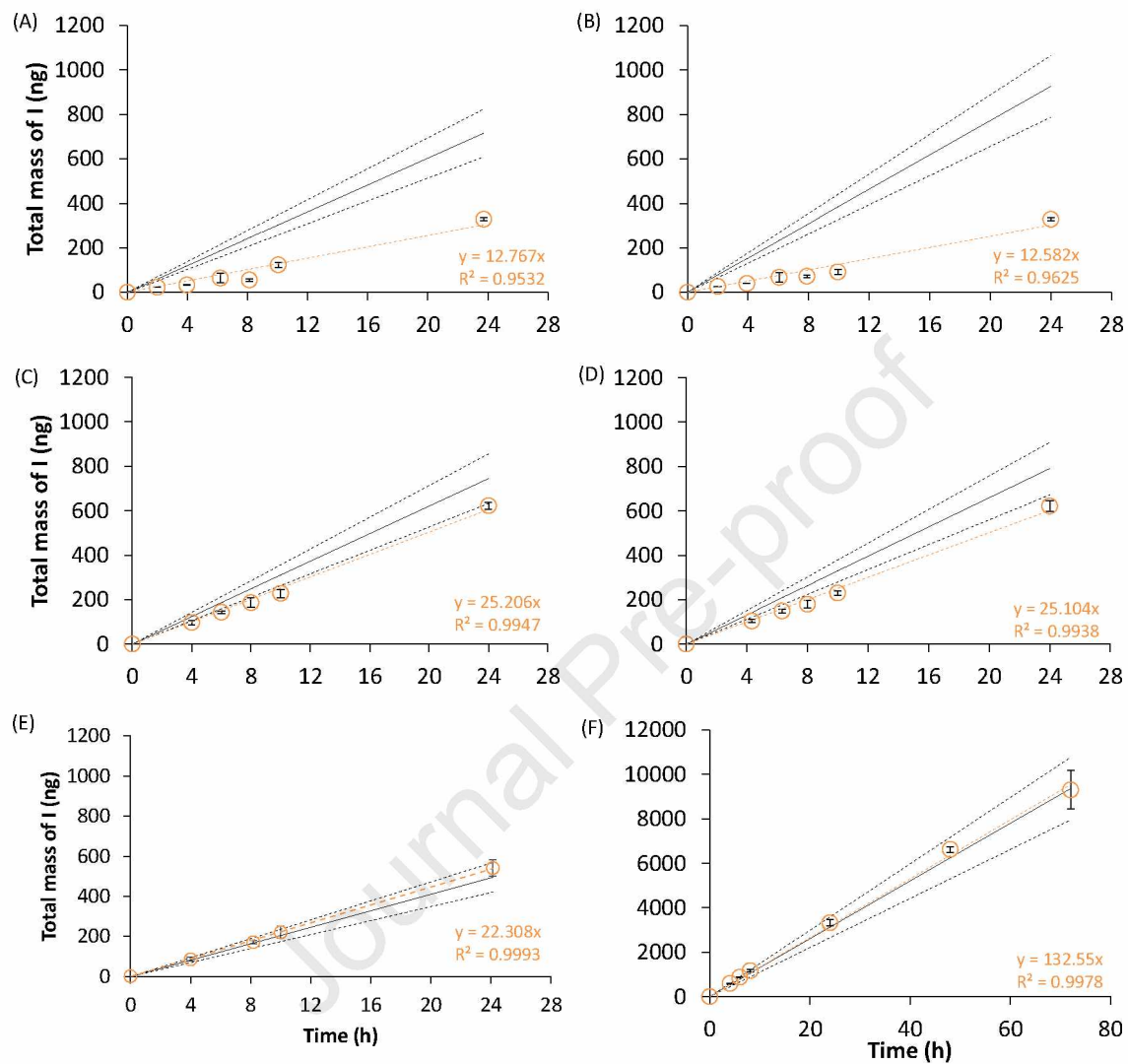


Figure 5



**Table caption**

Table 1: Continental water and seawater composition. Drinking-water physicochemical compositions provided in the bottle labels, and seawater was prepared according to Grasshoff et al. [62].

Table 2: Compilation of the experimental diffusion coefficients for  $\text{IO}_3^-$  and  $\text{I}^-$  at 25°C. Abbreviations:  $D^w$ : the diffusion coefficient in pure water;  $D^{\text{gel}}$ : the diffusion coefficient in AGE hydrogel;  $D^{\text{mdl}}$ : the diffusion coefficient in CA filter plus AGE hydrogel;  $D^{\text{eff}}$ : the effective diffusion coefficient measured by the DGT times-series method ( $[\text{NaCl}] = 10 \text{ mmol L}^{-1}$ ; pH  $\sim 5.5$ ); n.d.: not determined.



Table 1

Element/dissolved species	Volvic	Vittel	Seawater
Ca	0.29	5.99	13.6 mmol/L
Mg	0.33	1.73	114 mmol/L
Na	0.50	0.23	471 mmol/L
K	0.16	0.05	9.46 mmol/L
HCO <sub>3</sub> <sup>-</sup>	1.16	6.29	2.38 mmol/L
Cl <sup>-</sup>	0.38	0.23	675 mmol/L
SO <sub>4</sub> <sup>2-</sup>	0.08	4.16	28.2 mmol/L
NO <sub>3</sub> <sup>-</sup>	0.24	0.07	mmol/L
pH	7	7.6	8.22 mmol/L
dry residue	130	1084	mg/L
Salinity			34.8

Table 2

	Diffusion coefficient ( $\times 10^{-5} \text{ cm}^2 \text{ s}^{-1}$ )	
	$\text{IO}_3^-$	$\Gamma$
$D^w$	1.08 [63]	2.05 [63]
$D^{\text{gel}}$	1.19 (RSD = 5 %)	2.33 (RSD = 6 %)
$D^{\text{mdl}}$	0.87 (RSD = 5 %)	1.61 (RSD = 5 %)
$D^{\text{eff}}$	n.d.	1.20 (RSD = 6 %)

Journal Pre-proof

**Highlights:**

- A new DGT binding gel is proposed for selective iodide sampling.
- The diffusion coefficient of I species through agarose diffusive gel is reported.
- A DGT equation is developed to consider diffusive boundary layer and kinetic effects.
- The method was successfully applied to measure iodide concentrations in seawater.

Journal Pre-proof

**Declaration of interests**

The authors declare that they have no known competing financial interests or personal relationships that could have appeared to influence the work reported in this paper.

The authors declare the following financial interests/personal relationships which may be considered as potential competing interests:

Journal Pre-proof